ChemComm

COMMUNICATION

View Article Online
View Journal | View Issue

Cite this: *Chem. Commun.*, 2018, **54**, 9163

Received 7th July 2018,
Accepted 20th July 2018

DOI: 10.1039/c8cc05482g

rsc.li/chemcomm

An electro-responsive imprinted biosensor with switchable affinity toward proteins†

Yubo Wei, Qiang Zeng, Jianzhi Huang, Qiong Hu, Xinrong Guo and Lishi Wang *

We combined electro-responsive materials with molecular imprinted polymers (MIPs) to develop an electro-responsive imprinted biosensor for the first time. As an electric field controlled gate, the biosensor exhibits a novel self-cleaning ability, as well as switchable affinity toward proteins in aqueous media, based on a reversible structure change.

Molecular recognition materials, as a significant class of functional materials, have aroused much attention due to their important contribution to various fields of natural science. Traditional natural molecular recognition systems, including antibodies and enzymes, have shown molecular recognition properties and wide applications in protein purification,[1] sensors,[2] clinical diagnosis,[3] drug monitoring, and therapy.[4] However, owing to their fragile and flexible properties, it is difficult to modify molecular recognition materials for further functionalization.[5] Thus, to address this issue, molecular imprinted polymers (MIPs), which possess specific recognition sites for template molecules and act as promising artificial molecular materials, have been applied to various fields to replace natural antibodies.[6–10]

"Smart" or responsive polymers are materials that respond to applied chemical or physical stimuli, such as pH,[11] light,[12,13] temperature,[14] and electric fields,[15] and switch the surface structure and micro-morphology of materials, such as through expansion, elongation, contraction, and bending. By combining "smart" materials with MIPs, the developed materials exhibit superior switchable molecular recognition performances under external stimuli. Among these stimuli-responsive MIPs, pH-responsive MIPs containing ionizable groups are sensitive to changes in pH, and are capable of accepting or donating protons at a fixed pH value. This further causes changes to the hydrodynamic volume in the polymer chains by undergoing volume phase transitions from a compact state to a swelling state. However, the pH effect on these pH-responsive MIPs will be significantly weakened due to salt accumulation in the solution. In particular, salt accumulation greatly changes the electrolyte content of an electrolyte solution in electrochemical detections. Meanwhile, the process of pH response with external acids or alkalis is relatively tedious and time-consuming. These disadvantages are forecast to limit the applications and prospects of pH-responsive MIPs and it is thus necessary to develop a new method that makes the pH response of MIPs convenient and independent of external acids or alkalis.

Electro-responsive polymers (ERPs) can be capable of transforming an electric field into mechanical energy.[16–18] Therefore, ERPs have already attracted great interest in scientific and technological domains lately, such as for sensors and actuators, biomedical, and biomolecule adhesion applications,[19–23] because they have the unique advantages of automatic and programmed control, as well as remote control. In addition, the hydrogen evolution reaction can be triggered by an electric field stimulus, providing the functionality of pH control. By applying this property to molecular recognition systems, it offers a useful strategy to processes of electro-responsive molecular recognition under an electric field stimulus.

Herein, a novel electric field stimuli responsive MIP biosensor with a switchable affinity toward the template protein of human serum albumin (HSA) was developed for the first time (Scheme 1) on a glassy carbon electrode (GCE). For the MIP, *N*,*N*′-dimethylaminoethylmethacrylate (DMAEMA) was used as an electro-responsive monomer to control the release and uptake of the template protein with a proper applied potential. In particular, the protonated and positively charged tertiary amine groups of DMAEMA can be efficiently changed to their deprotonated and uncharged state by the hydrogen evolution reaction under an electric field stimulus, *e.g.* a voltage of −1.2 V, in water. This results in the removal of the template protein from the imprinted materials without the help of washing solvents and produces sensing nanocavities for the target protein. The reverse is

School of Chemistry and Chemical Engineering, South China University of Technology, Guangzhou 510641, People's Republic of China.
E-mail: wanglsh@scut.edu.cn

† Electronic supplementary information (ESI) available. See DOI: 10.1039/c8cc05482g

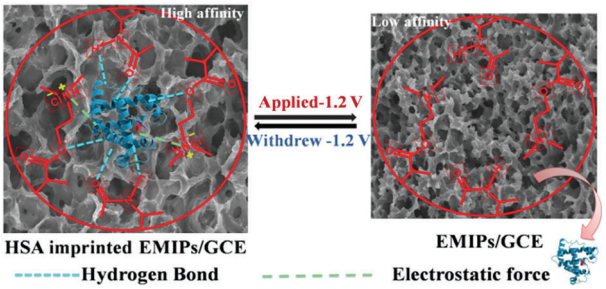

Scheme 1 Electro-responsive properties of the EMIPs/GCE biosensor.

achieved by withdrawing the voltage. Therefore, the recognition sites can be simply controlled by structural changes of the EMIP monomers only at certain applied and withdrawn voltages.

An electro-responsive imprinted biosensor (EMIPs/GCE), an electro-responsive non-imprinted biosensor (ENIPs/GCE), and an imprinted biosensor without the addition of DMAEMA (MIPs/GCE without DMAEMA) were synthesized according to radical polymerization (Scheme S1 in ESI†), and were fully characterized by FT-IR and cyclic voltammetry (CV). As shown in Fig. S1 (ESI†), after polymerization, the peaks at 3300 and 1520, and 1645 and 1156 cm^{-1} appeared and are attributed to the N–H stretching vibration and the amide carbonyl bending vibration of *N*-isopropylacrylamide (NiPAAm) monomer, and the C=O stretching vibration and the C–O symmetric stretching of esters in the DMAEMA monomer.[24] The CV responses of a bare GCE and the modified GCE were further used to certify the formation of the HSA imprinted EMIPs/GCE. Compared with the bare GCE (curve a, Fig. 1A), the peak current of $[Fe(CN)_6]^{3-/4-}$ was obviously decreased after modification of the HSA imprinted EMIP film on the GCE surface (curve b, Fig. 1A). This is due to the barely conductive and compact properties of the HSA imprinted EMIP film. The results mean that we have successfully prepared imprinted films on the GCE.

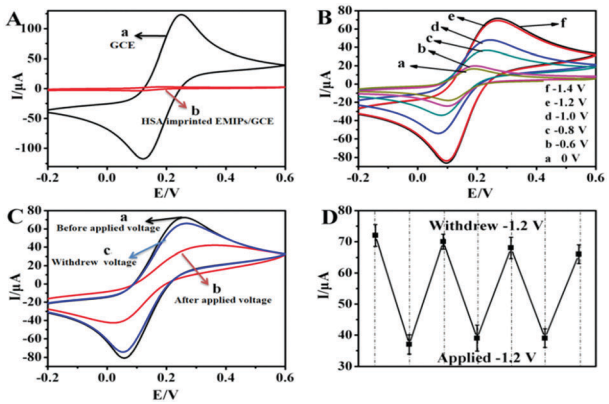

Fig. 1 CV responses of (A) the bare GCE (a) and HSA imprinted EMIPs/GCE (b); (B) the HSA imprinted EMIPs/GCE removal of HSA under different potentials for 150 s and subsequent withdrawal of the voltage, before being kept for 55 min in pH 5.5 PBS; (C) the EMIPs/GCE before (curve a) and after (curve b) the application of −1.2 V for 150 s and subsequent withdrawal of the voltage, before being kept for 55 min (curve c); (D) variation of the CV I_{pc} of the EMIPs/GCE for the electro-switch across three cycles in a pH 5.5 PBS buffer containing 0.1 mol L^{-1} KCl and 5 mmol L^{-1} $[Fe(CN)_6]^{3-/4-}$.

In order to illustrate the self-cleaning efficiency of HSA from the imprinted EMIPs/GCE under an electric field stimulus, the release of HSA has been investigated at different applied voltages (*i.e.* −0.6 V, −0.8 V, −1.0 V, −1.2 V, and −1.4 V for 150 s) and times (50 s, 100 s, 150 s, and 200 s at −1.2 V) by CV of $[Fe(CN)_6]^{3-/4-}$. Before these measurements, the biosensor was put on standby for 55 min in pH 5.5 PBS without applied potential for comparison with the blank experiment, which was conducted without electric voltage (hereafter denoted 0.00 V). As shown in Table S1 (ESI†) and Fig. 1B, there are no changes to the current when a potential of −0.6 V is applied to the HSA imprinted EMIPs/GCE (entry 2, curve b). Subsequently, the current starts to increase gradually when the applied potential varies from −0.8 V to −1.2 V, and then becomes almost constant by increasing the voltage to −1.4 V (entries 3–6, curves c–f). With an increase in time under −1.2 V, the current increases first and remains basically unchanged (entries 7, 8, 5, and 9). The increase in the current with an applied potential between −0.8 V to −1.2 V is mainly due to the hydrogen evolution reaction on the HSA imprinted EMIPs/GCE. The reaction facilitates an increase in the local OH^- concentration, which turns the tertiary amine groups of poly DMAEMA (p-DMAEMA) in the EMIPs to their uncharged and deprotonated states. The hydrogen bonding and electrostatic interactions between the monomers and templates can be suppressed, resulting in the removal of the templates from the HSA imprinted EMIPs/GCE and the production of sensing nanocavities for the target proteins, causing the higher CV response. In contrast, the templates have already been fully eliminated beyond applied potentials of −1.2 V for 150 s and there are no significant changes in the current. For these purposes, −1.2 V for 150 s are adopted as the optimal self-cleaning conditions. For comparison, the optimal voltage and time are applied to the HSA imprinted MIPs/GCE without DMAEMA under the same conditions. As shown in Table S1 (entries 10 and 11) (ESI†), the applied voltage does not substantially affect the current due to the lack of electro-responsive groups in the imprinting processes.

However, Fig. 1B is not reflective of the cavity volume changes of the EMIP film. Without the standby time at zero potential and the presence of HSA, the redox peak currents of $[Fe(CN)_6]^{3-/4-}$ from the EMIPs/GCE also depend upon the applied potential and time (Fig. S2A and B, ESI†). In particular, at the optimal applied voltage and time of −1.2 V and 150 s, the current showed a dramatic reduction (curve b, Fig. 1C). In contrast, with a standby time of 55 min after withdrawing the voltage, the redox peak current of $[Fe(CN)_6]^{3-/4-}$ in the CV response (curve c, Fig. 1C) can be nearly fully recovered. Therefore, these observations demonstrate that the EMIPs/GCE conducts a reversible structural change (from a less compact structure to a compact structure) with repeatable withdrawn and applied voltage, exhibiting a switchable ON–OFF phenomenon owing to its electro-responsive properties (Fig. 1D). This also coincides with the results of the electrochemical impedance spectroscopy (EIS) in Fig. S3 (ESI†). Meanwhile, the redox peak

currents of $[Fe(CN)_6]^{3-/4-}$ under −1.2 V for 150 s, as well as the time taken to restore the current to its initial state at different pH, are shown in Fig. S2C (ESI†). This result provides strong proof that external electro-stimulus signals can be effectively converted to electrochemical signals by the EMIPs/GCE with rapid electrochemical switching properties and easily reversible cyclicity.

With the assistance of SEM, it has been confirmed that the electro-stimuli responsive properties of the EMIPs/GCE are the consequence of the structural change of the electro-sensitive p-DMAEMA part of the EMIP films. As a consequence, the removal of HSA is not only caused by the change in the recognition sites, but also by the change in the cavity volume in the EMIP film. Both effects are triggered by electric field stimulation, causing the template molecules to be completely removed. At pH 5.5, the film exhibited large holes or cavities with pore diameters of 8 μm (Fig. 2A and B). When −1.2 V was applied, the pore diameters became more compact and much smaller, decreasing to 4 μm (Fig. 2C and D). With a standby time of 55 min after withdrawing the voltage, the surface structure of the EMIP film can be nearly fully recovered (Fig. 2E and F). The pK_a of p-DMAEMA was reported to be approximately 7.0.[25] At pH 5.5, the tertiary amine groups of the p-DMAEMA part in the EMIPs were protonated and positively charged. The repulsive interaction between the positively charged groups causes swelling of the EMIP films on the electrode surface. At this point, the diffusion of the probe through the films to the electrode surface becomes more convenient, leading to a higher CV response and weaker interfacial electron transfer resistance (ETR). In contrast, when −1.2 V was applied to the EMIPs/GCE, the protonated and positively charged tertiary amine groups of p-DMAEMA can be changed by the hydrogen evolution reaction. This reaction facilitates local pH variation, making the protonated and positively charged amine groups of p-DMAEMA become uncharged and deprotonated, producing a compact and contracted structure, limiting the diffusion of the probe to the electrode surface and leading to a weaker CV response and stronger ETR. For comparison, the MIP film without DMAEMA exhibited pore diameters of 2 μm at pH 5.5 (Fig. S4A and B, ESI†). When applying the voltage, the pore diameter still remained the same (Fig. S4C and D, ESI†). This result coincides with the observations from the CV (Fig. S5, ESI†).

The adsorption time for rebinding the templates is a significant parameter for judging the properties of the EMIPs/GCE. Fig. 3A illustrates the DPV peak current variation (ΔI) of $[Fe(CN)_6]^{3-/4-}$ for the imprinted and non-imprinted biosensor after and before interaction with 0.5 mL of 1.0 μmol L^{-1} HSA with different incubation times. It was found that the ΔI of the probe increased sharply in the first 12 min and then reached a steady-state current, which means that HSA has almost completely rebound to the imprinting sites after 12 min. For the non-imprinted biosensor, however, the binding capacity is obviously less than that of the imprinted sensor, because of a lack of specific adsorption sites. The binding isotherms of HSA were assessed for the EMIPs/GCE within the scope of the effective concentration from 0.05 to 5.0 μmol L^{-1}. With an increase in the HSA concentration, the adsorption amounts of HSA onto the EMIPs/GCE also increased and reached a saturation value at 1.0 μmol L^{-1}. For the EMIPs/GCE, there are two linear regression equations including lower concentrations and higher concentrations, which suggests two types of affinity site, of high and low affinity, in the EMIPs/GCE (Fig. 3B). In contrast, the ENIPs/GCE was insensitive to HSA because of the lack of recognition sites in the nanocavities of the ENIPs/GCE. The practicability of the proposed biosensor was realized by extracting HSA from a complex serum sample. As shown in Table S2 and Scheme S2 (ESI†), the EMIPs/GCE was capable of extracting HSA from a complex serum sample with excellent recovery, which was determined by a UV-vis spectroscopic method.[14] The results implied that the obtained biosensor is able to perform as an effective, precise, and reliable sensing platform for extracting HSA from complex serum samples.

To assess the selectivity of the EMIPs/GCE for HSA (MW 66 kDa), human immunodeficiency virus p24 (HIV-p24: 24 kDa), human chorionic gonadotropin (HCG: 36 kDa), Bovine serum albumin (BSA: 66 kDa), α-fetoprotein (AFP: 66 kDa), and carcino-embryonic

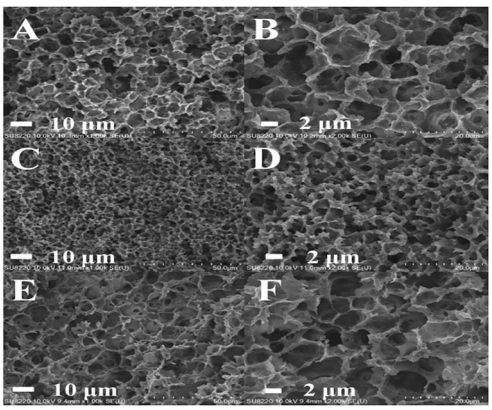

Fig. 2 SEM of the EMIP film prepared on the GCE surface before (A and B) and after applying −1.2 V for 150 s (C and D). Subsequently, the voltage was withdrawn, and the sample was kept for 55 min (E and F) at 25 °C in a pH 5.5 PBS buffer.

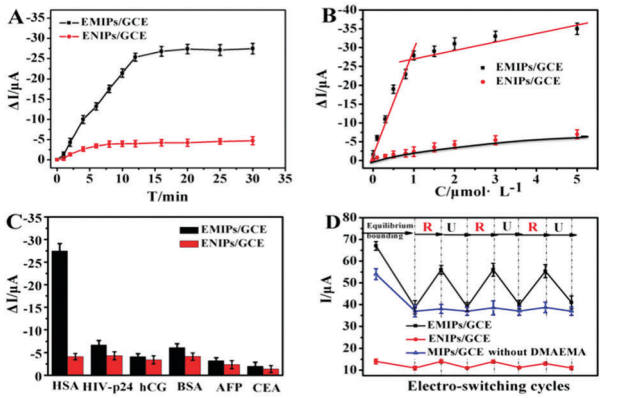

Fig. 3 EMIPs/GCE and ENIPs/GCE (A) incubation times; (B) calibration curves toward HSA standards in a pH 5.5 PBS buffer; (C) selectivity tests; (D) electro-driven release (R) and uptake (U) of HSA by the EMIPs/GCE, ENIPs/GCE, and MIPs/GCE without DMAEMA.

antigen (CEA: 180 kDa) were chosen as potential interferents, owing to the fact that they have some existent protein with a similar structure and cover a wider molecular weight in serum. As shown in Fig. 3C, the ΔI of $[Fe(CN)_6]^{3-/4-}$ is much higher than that of the other interferents for the EMIPs/GCE at 0.5 mL of 1.0 μmol L^{-1} HSA. In contrast, there were almost no noticeable distinctions between HSA and the analogues for the ENIPs/GCE as a result of the lack of specific recognition sites. The proposed result is proven to have statistical stability, as well as satisfying the selectivity for the template HSA.

Accompanied by the self-cleaning process, the EMIPs/GCE can exhibit highly efficient release and uptake of 0.5 mL of 1.0 μmol L^{-1} HSA under alternating applied and withdrawn −1.2 V, respectively. As shown in Fig. 3D, the DPV peak current of $[Fe(CN)_6]^{3-/4-}$ decreased from 67 μA to 40 μA after the adsorption equilibrium. At this time, the imprint sites and structure size of the nanocavities are most complementary to the template. Subsequently, the application of −1.2 V to the HSA imprinted EMIPs/GCE causes the DPV peak current to increase from 40 μA to 56 μA, as a result of releasing the bound HSA into the solution. On the contrary, withdrawing −1.2 V causes the rebinding of HSA back into the EMIPs/GCE, with the DPV peak current reduced from 56 μA to 41 μA. At this moment, the imprinted cavities and specific recognition sites for HSA in the EMIPs/GCE are re-generated. For the rebinding of HSA, the receptors provide efficient hydrogen bonding sites and electrostatic force in this state. This observation was confirmed by mercury intrusion porosimetry. As shown in Fig. S6 (ESI†), the EMIP films before the application of voltage and after the removal of the voltage have similar cumulative intrusion curves and pore size distributions, which means these two samples have similar pore structures, as confirmed by SEM (Fig. 2A, B, E and F). Therefore, the electro-responsive rebinding capacity principally originates from electro-dependent volume phase transitions, as well as the two states of the tertiary amine groups in the p-DMAEMA part of the EMIPs. During these processes, the EMIPs/GCE displayed excellent reversibility and favourable stability after three cycles. However, the MIPs/GCE without DMAEMA has shown little current change under the same conditions. This is due to the lack of electro-responsive groups in the imprinting processes. Moreover, the release and uptake of HSA for the ENIPs/GCE only causes negligible current changes under the same procedure.

In conclusion, a selective and sensitive electro-responsive MIP biosensor was designed and synthesized for the first time. An electro-responsive molecule of DMAEMA was used as a functional monomer for the targeting of HSA protein. The receptor-binding ability toward the template protein was controlled by applying and withdrawing the voltage. Based on the above advantages, the proposed biosensor exhibited novel self-cleaning behaviour toward the template upon the application of an electric field at room temperature without the help of washing solvents; moreover, electro-responsive MIPs are employed as electrical gates to extract the HSA protein from serum sample mixtures with good stability and cyclic performance. This work offers a promising supplement for stimuli-responsive MIP sensing applications, such as reusable sensors, cell adhesives, and analytical tools.

Conflicts of interest

There are no conflicts to declare.

Notes and references

1 A. Sassolas, B. D. Leca-Bouvier and L. J. Blum, *Chem. Rev.*, 2008, **108**, 109.
2 Y. Jiang, M. L. Shi, Y. Liu, S. Wan, C. Cui, L. Q. Zhang and W. H. Tan, *Angew. Chem., Int. Ed.*, 2017, **56**, 11916.
3 K. Tawa, F. Kondo, C. Sasakawa, K. Nagae, Y. Nakamura, A. Nozaki and T. Kaya, *Anal. Chem.*, 2015, **87**, 3871.
4 T. A. Waldmann, *Science*, 1991, **252**, 1657.
5 Y. Kitayama and M. Isomura, *Chem. Commun.*, 2018, **54**, 2538.
6 Z. J. Zhang, Y. J. Guan, M. Li, A. D. Zhao, J. S. Ren and X. G. Qu, *Chem. Sci.*, 2015, **6**, 2822.
7 R. Horikawa, H. Sunayama, Y. Kitayama, E. Takano and T. Takeuchi, *Angew. Chem., Int. Ed.*, 2016, **55**, 13023.
8 G. Wulff, *Angew. Chem., Int. Ed. Engl.*, 1995, **34**, 1812.
9 J. Bognár, J. Szűcs, Z. Dorkó, V. Horváth and R. E. Gyurcsányi, *Adv. Funct. Mater.*, 2013, **23**, 4703.
10 T. S. Metzger, R. T. Vered, H. B. Albada and I. Willner, *Adv. Funct. Mater.*, 2015, **25**, 6470.
11 X. Chen, J. Gao, B. Song, M. Smet and X. Zhang, *Langmuir*, 2010, **26**, 104.
12 Y. Wei, Q. Zeng, S. Bai, M. Wang and L. Wang, *ACS Appl. Mater. Interfaces*, 2017, **9**, 44114.
13 Y. Wei, Q. Tang, C. Gong and M. H. W. Lam, *Anal. Chim. Acta*, 2015, **900**, 10.
14 Y. Wei, Q. Zeng, Q. Hu, M. Wang, J. Tao and L. Wang, *Biosens. Bioelectron.*, 2018, **99**, 136.
15 X. Ying, Y. Wang, J. Liang, J. Yue, C. Xu, L. Lu, Z. Xu, J. Gao, Y. Du and Z. Chen, *Angew. Chem., Int. Ed.*, 2014, **53**, 12436.
16 N. H. Nassab, D. Samanta, Y. Abdolazimi, J. P. Annesb and R. N. Zare, *Nanoscale*, 2017, **9**, 143.
17 A. P. Jou, P. Micheletti, F. Estrany, L. J. del Valle and C. Alemán, *Adv. Healthcare Mater.*, 2017, **6**, 1700453.
18 H. Zeng, Y. Zhang, S. Mao, H. Nakajima and K. Uchiyama, *J. Mater. Chem. C*, 2017, **5**, 5877.
19 T. Manourasa and M. Vamvakaki, *Polym. Chem.*, 2017, **8**, 74.
20 J. Lu, S. G. Kim, S. Lee and I. K. Oh, *Macromol. Chem. Phys.*, 2011, **212**, 635.
21 S. S. Kim and C. D. Kee, *Int. J. Precis. Eng. Manuf.*, 2014, **15**, 315.
22 W. Kunchornsup and A. Sirivat, *Sens. Actuators, A*, 2014, **220**, 249.
23 O. V. Borisova, L. Billon, R. P. Richter, E. Reimhult and O. V. Borisov, *Langmuir*, 2015, **31**, 7684.
24 G. Liu, D. Wang, F. Zhou and W. Liu, *Small*, 2015, **11**(23), 2807.
25 G. Gurdag and B. Kurtulus, *Ind. Eng. Chem. Res.*, 2010, **49**, 12675.

